

Sodium-Centered Dodecanuclear Co(II) and Ni(II) Complexes with 2-(Phosphonomethylamino)succinic Acid: Studies of Spectroscopic, Structural, and Magnetic Properties

Andriy O. Gudima,^{*,†} Ganna V. Shovkova,[†] Olena K. Trunova,[†] Fernande Grandjean,^{‡,§} Gary J. Long,^{*,§} and Nikolay Gerasimchuk^{*,||}

[†]V. I. Vernadsky Institute of General and Inorganic Chemistry, Ukrainian National Academy of Sciences, 03680, Kyiv 142, Akademika Palladina Ave. 32/34, Ukraine

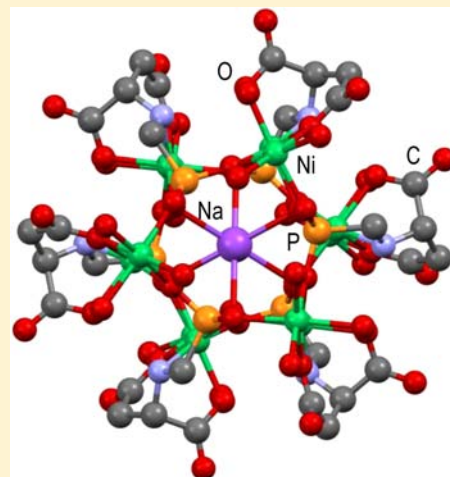
[‡]Faculty of Sciences, B6, University of Liège, B-4000 Sart-Tilman, Belgium

[§]Department of Chemistry, Missouri University of Science and Technology, University of Missouri, Rolla, Missouri 65409-0010, United States

^{||}Department of Chemistry, Temple Hall 456, Missouri State University, Springfield, Missouri 65897, United States

Supporting Information

ABSTRACT: Two new isostructural cobalt(II) and nickel(II) polynuclear complexes with 2-(phosphonomethyl)aminosuccinic acid, H₄PMAS, namely, Na [Co₁₂(PMAS)₆(H₂O)₁₇(OH)]·xH₂O, 1·xH₂O, and Na [Ni₁₂(PMAS)₆(H₂O)₁₇(OH)]·xH₂O, 2·xH₂O, have been synthesized for the first time from aqueous solutions and studied by single crystal X-ray diffraction, infrared, and UV–visible diffuse reflectance spectroscopy; TG/DTA analysis; and magnetochemistry. Both **1** and **2** crystallize in the rhombohedral crystal system with the R $\bar{3}$ space group with 1/6 of the Co₁₂(PMAS)₆ or Ni₁₂(PMAS)₆ moieties in the asymmetric unit. The X-ray refinements reveal the presence of 18 water sites, but unit cell charge balance requires that one water molecule must be an OH[−] anion, an anion which is disordered over the 18 sites. The PMAS^{4−} ligand forms two five-membered and one six-membered chelation ring. Both **1** and **2** contain 24-membered metallacycles as a result of the bridging nature of the PMAS^{4−} ligands. The resulting three-dimensional structures have one-dimensional channels with a sodium cation at the center of symmetry. The temperature dependence of the magnetic susceptibility reveals the presence of weak antiferromagnetic exchange coupling interactions in both **1** and **2**. Two exchange coupling constants, $J_1 = -15.3(7) \text{ cm}^{-1}$ and $J_2 = -1.06(2) \text{ cm}^{-1}$ with $S_1 = S_2 = 3/2$ for the Co(1)⋯Co(1) and Co(1)⋯Co(2) exchange pathways, respectively, are required for **1**, and $J_1 = -1.17(6) \text{ cm}^{-1}$ and $J_2 = -4.00(8) \text{ cm}^{-1}$ with $S_1 = S_2 = 1$ for the Ni(1)⋯Ni(1) and Ni(1)⋯Ni(2) exchange pathways, respectively, are required for **2**, in order to fit the temperature dependence of the observed magnetic susceptibilities.



INTRODUCTION

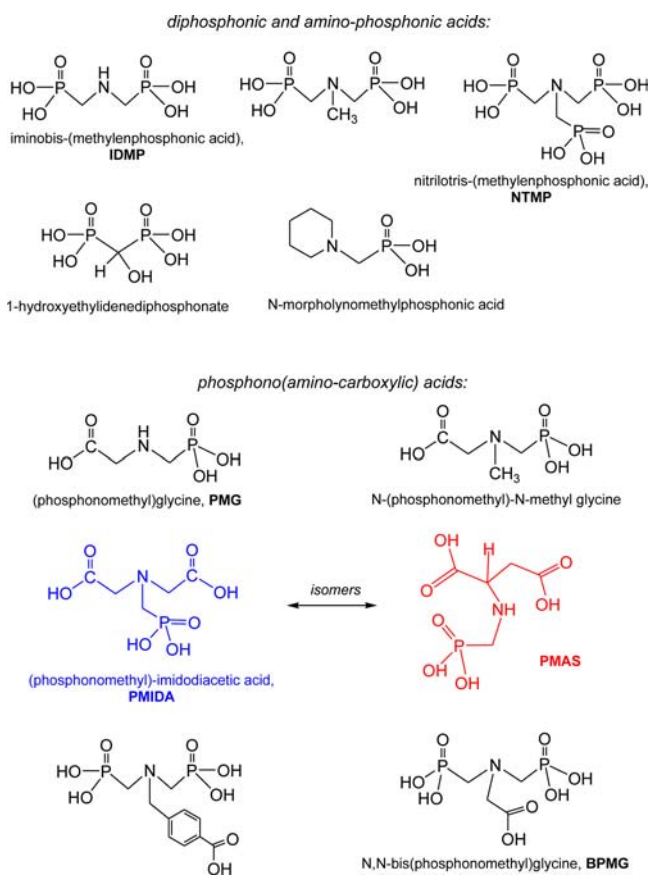
The multifunctional aminocarboxylic and phosphono-aminocarboxylic acids serve as polydentate ligands and yield transition metal complexes that are widely used in engineering, industry, agriculture, and medicine.^{1–3} The most common former compounds are nitrilotriacetic acid (NTA), 1,2-ethylenediaminetetraacetic acid (EDTA), and diethylenetriaminepentaacetic acid (DTPA). Because of their strong chelating interaction with metal cations, these ligands are potentially useful for countering the adverse effects of some cations on ecosystems and biological systems.^{4–7} Phosphorylated aminocarboxylate ligands are also known to be strong chelating agents and to form coordination compounds of various compositions, including polynuclear complexes, of high stability with most metal cations.^{8–12} These were found to be better ligands that deliver stronger acidity,

greater steric flexibility, a variety of binding modes, and donor atoms superior to that in their parent aminocarboxylic acids. Formulas of the most studied recently phosphorylated aminocarboxylic acids are presented in Scheme 1 along with their most commonly used abbreviations. There are three most investigated aminocarboxyphosphonate compounds, such as, *N*-(phosphonomethyl)glycine or glyphosate, H₃PMG, H₃CN(CH₂COOH)CH₂PO₃H₂, herein referred to as H₃PMG, while *N*-(phosphonomethyl)iminodiacetic acid, H₂O₃PCH₂N(CH₂COOH)₂, is herein referred to as H₄PMIDA, and *N,N*-bis(phosphonomethyl)glycine, (H₂O₃PCH₂)₂NCH₂COOH, is herein referred to as H₅BPMG.^{4,10,12} A new structural isomer of

Received: February 11, 2013

Published: June 10, 2013

Scheme 1. Formulas of Studied up to Date Amino-Carboxylic Phosphonic and Diphosphonic Acids



H_4 PMIDA—*N*-(phosphonomethyl)aminosuccinic acid—indicated in red and further abbreviated as H_4 PMAS (Scheme 1), was obtained and characterized for the first time.

Undoubtedly the combination of different functional groups, such as carboxyl, phosphonic, and amine groups in one ligand, yields novel compounds with unique properties. Many of these compounds are large poly(multinuclear) complexes that exhibited fascinating structures and unusual properties. Recent structural studies of the above and related ligands and complexes include the Cu-*N*-(phosphonomethyl)glycine complex, which was the first reported crystal structure.¹³ The polymeric cobalt(II) complex with this ligand, which contains a protonated nitrogen, has also been investigated.¹⁴ In $Na_3[Co^{III}(PMG)_2] \cdot 11H_2O$ ¹⁵ and $[Ni^{II}(HPMG)_2] \cdot [Ni(H_2O)_6] \cdot 3.3H_2O$, all the cationic coordination sites are filled by all the donors of glyphosate.¹⁶ The *N,N*-bis-(phosphonomethyl)glycine ligand forms complexes with several different structures.^{17–19} Most of the *N*-(phosphonomethyl)limino)diacetates contain three five-membered chelating rings coordinating the metal cations with the nitrogen and oxygen donors of two carboxylic and phosphonic groups.^{20–26} Some complexes form polymeric structures via the terminal carboxylic acid of H_4 PMIDA in the absence of any coordination by imino groups.^{17,27}

A new structural isomer of H_4 PMIDA, namely *N*-(phosphonomethyl)aminosuccinic acid, $H_2O_3PCH_2NHCH(COOH)CH_2COOH$, herein H_4 PMAS, has been synthesized recently in our laboratory. The lower symmetry of H_4 PMAS, as compared with H_4 PMIDA, removes the structural equivalence of

portions of the ligand and, thus, facilitates the conformational studies of its coordination complexes.

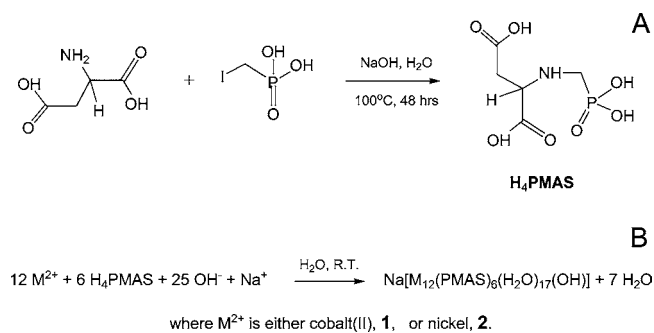
Herein, we present the crystal structures, and the spectral and magnetic properties of two new isostructural complexes of H_4 PMAS, namely, $Na[Co_{12}(PMAS)_6(H_2O)_{17}(OH)]$, **1**, and $Na[Ni_{12}(PMAS)_6(H_2O)_{17}(OH)]$, **2**, complexes that contain two crystallographically unique cobalt(II) or nickel(II) ions or six each, for a total of 12, and exhibit a unique architecture in which the sodium ion is in the center of both complexes and is responsible for holding together six ligating metal dications.

EXPERIMENTAL SECTION

Materials and Methods. Iodomethylphosphonic acid has been prepared by acidic hydrolysis of its ester according to a previously reported procedure.²⁸ All the chemicals used were of analytical reagent grade and were obtained from Aldrich and used without further purification. The carbon, hydrogen, and nitrogen content were obtained using the combustion method with a Perkin-Elmer CHN 2400 elemental analyzer. The phosphorus content was measured by X-ray fluorescence spectroscopy with an EXPERT 3L spectrometer. The metal contents were determined by atomic absorption with a Philips Pye Unicam 8000 atomic absorption spectrophotometer. The pH of the solutions was measured with a Mettler Delta 350 pH meter.

Synthesis of 2-(Phosphonomethyl)aminosuccinic Acid. 2-(Phosphonomethyl)aminosuccinic acid, $HOOC-CH_2-CH(COOH)-NH-CH_2PO_3H_2$, herein H_4 PMAS, was synthesized by alkylation of *D,L*-aspartic acid with iodomethylphosphonic acid in strongly alkaline aqueous media at 100 °C for 48 h as depicted in

Scheme 2. Formulas of the Amino-Carboxylic Phosphonic and Diphosphonic Acids Studied to Date



Scheme 2A. NMR data: 1H (D_2O) δ (ppm): 3.07 (dd, $^3J_{HH} = 5.0$ Hz, $^3J_{HH} = 5.8$ Hz); 3.27 (dd, $^2J_{HP} = 12.4$ Hz, $^2J_{HP} = 13.0$ Hz); 4.18 (ps-t = dd, $^3J_{HH} = 5.0$ Hz, $^3J_{HH} = 5.8$ Hz). ^{31}P (D_2O) δ (ppm): 10.36 (t, $^2J_{HP} = 12.4$ Hz). ^{13}C (D_2O) δ (ppm): 33.13 (s) CH_2COO ; 42.98 (d, $^1J_{CP} = 137.9$ Hz) CH_2P ; 58.36 (d, $^3J_{CP} = 7.3$ Hz) CH ; 171.21 (s) CH_2COO ; 173.72 (s) $CHCOO$. Anal. Calcd. for $C_5H_{10}NO_7P$, calculated (found, %): C, 26.44 (26.67); H, 4.41 (4.48); N, 6.17 (6.24); P, 6.64 (6.38). The acid is well soluble in water, and its stepwise deprotonation constants have been measured at two different concentrations using two different methods (Supporting Information, S1 and S2).

The synthesis of metal derivatives—compounds **1** and **2**—was carried out in aqueous solutions at 2:1 metal to ligand ratio at pH \sim 5 as shown in Scheme 2B.

Synthesis of $Na[Co_{12}(PMAS)_6(H_2O)_{17}(OH)] \cdot 2H_2O$, further $1 \cdot xH_2O$. Cobalt(II) chloride, 2 mmol, and 2-(phosphonomethyl)aminosuccinic acid, 1 mmol, solutions each in 10 mL of distilled water were mixed together at room temperature. The pH of the resulting strongly acidic solution was adjusted to 5 by the dropwise addition of a 1 M NaOH solution, and the reaction mixture was subsequently heated for 40 min at 50 °C on a water bath. The resulting solution was transferred in a beaker that was placed in a closed vessel containing absolute ethanol which slowly vapor-diffused into the solution of the

Table 1. Crystal Data and Structures Refinement for 1 and 2

parameter	1, Na[Co ₁₂ (PMAS) ₆ (H ₂ O) ₁₇ (OH)]	2, Na[Ni ₁₂ (PMAS) ₆ (H ₂ O) ₁₇ (OH)]
empirical formula	NaCo ₁₂ C ₃₀ H ₇₁ N ₆ P ₆ O ₆₀	NaNi ₁₂ C ₃₀ H ₇₁ N ₆ P ₆ O ₆₀
fw, g/mol	2391.933	2389.251
crystal size, mm	0.17 × 0.15 × 0.14	0.17 × 0.13 × 0.13
cryst syst	rhombohedral	rhombohedral
space group	R $\bar{3}$	R $\bar{3}$
<i>a</i> , Å	13.4686(2)	13.3789(2)
α , deg	104.186(1)	103.810(1)
<i>V</i> , Å ³	2172.13(6)	2144.42(6)
<i>Z</i>	1	1
<i>D</i> _{calc} , g cm ⁻³	1.829	1.851
μ , mm ⁻¹	2.447	2.792
<i>T</i> , K	173(2)	173(2)
<i>F</i> (000)	1198	1210
θ range, deg	1.65 - 26.38	1.65 - 26.43
range of <i>h, k, l</i>	-16→16, -16→16, -16→16	-11→16, -16→16, -16→15
GOF	1.045	1.006
final <i>R</i> indices	<i>R</i> ^a = 0.0490 1	<i>R</i> ^a = 0.0373 1
<i>I</i> > 2 σ (<i>I</i>)	<i>R</i> ^b = 0.1230 <i>w</i>	<i>R</i> ^b = 0.0809 <i>w</i>
<i>R</i> indices (all data)	<i>R</i> ^a = 0.0712 1	<i>R</i> ^a = 0.0591 1
	<i>R</i> ^b = 0.1309 <i>w</i>	<i>R</i> ^b = 0.0858 <i>w</i>
largest peak/hole, e ⁻	0.539/-1.031	0.428/-0.604

$${}^aR_1 = \sum |F_o - F_c| / \sum |F_o|, {}^bR_w = [\sum w(F_o^2 - F_c^2)^2 / \sum wF_o^2]^{1/2}.$$

complex at room temperature. During a period of two weeks, small pink crystals were formed upon this slow diffusion; the crystals were then removed by filtration, washed with water, and air-dried to yield 51% of 1·2H₂O. Anal. Calcd. for NaCo₁₂C₃₀H₇₃N₆P₆O₆₂, calculated (found, %): C, 14.82 (15.18); H, 3.08 (2.88); N, 3.46 (3.65); P, 7.66 (7.14); Co, 29.12 (29.11); Na, 0.95 (0.91).

Synthesis of Na[Ni₁₂(PMAS)₆(H₂O)₁₇(OH)]·2H₂O, further 2·xH₂O. This complex was prepared by the same procedure as described above for complex 1 by using a nickel(II) sulfate solution. Light green crystals of 2·2H₂O were isolated in 38% yield. Anal. Calcd. for NaNi₁₂C₃₀H₇₅N₆P₆O₆₂, calculated (found, %): C, 14.84 (15.38); H, 3.09 (3.14); N, 3.46 (3.45); P, 7.67 (7.28); Ni, 29.04 (29.03); Na, 0.95 (0.90).

Both isolated metallophosphonates, 1·2H₂O and 2·2H₂O, are air-stable with respect to oxidation of the phosphonate ligand but slowly dehydrate losing the outer-sphere crystallization water at room temperature; both complexes are insoluble in common organic solvents.

Physical Methods and Measurements. Potentiometric titrations of H₄PMAS were performed in 0.01 and 0.001 M water solutions (1.5 mL total volume) using a MOLSPIN automatic titrator with a Russel CMAW 711 microcombined glass electrode (KCl aqueous solution was replaced with 0.1 M NaNO₃) at constant temperature (20 °C) and ionic strength (0.1 M NaNO₃) using 0.1 M NaOH as the titrant. The protonation constants were calculated using CLINP 2.1 and SUPERQUAD programs. The IR spectra were obtained at room temperature with a Karl Zeiss Specord M80 spectrophotometer over the range of 400 to 4000 cm⁻¹ by using KBr pellets. The solid state UV-visible spectra were obtained with a Karl Zeiss Specord M40 spectrophotometer over the range of 300 to 900 nm with the MgO powdery sample used as a reflectance standard. The NMR spectra were recorded for H₄PMAS at 20 ± 2 °C by using a Bruker Avance 400 spectrometer with an 85% H₃PO₄ solution as an external standard for ³¹P and ¹H spectra. The TG/DTA measurements were carried out on a Perkin-Elmer STA 600 thermoanalyzer under N₂ protection at a 20°/min heating rate in the range 50–550 °C, while for the range 550–950 °C the rate was 40°/min. For complex 1, thermo-gravimetric measurements were also conducted in the oxygen atmosphere.

Single Crystal X-Ray Structure Determinations. The X-ray quality rhombic-shaped pink and green single crystals of 1·2H₂O and 2·2H₂O, respectively, were grown from the aqueous solutions upon diffusion of ethanol and slow evaporation. Three-dimensional sets of

reflection intensities were obtained at 100 K on a Bruker SMART APEX 2 diffractometer with 0.71073 Å Mo K α radiation and a graphite monochromator by using the ω - and φ -scan techniques. Semi-empirical intensity corrections for absorption, polarization, and the Lorentz effect were carried out by using the SADABS program.²⁹ The structure was solved by direct methods and refined by the full matrix least-squares method on *F*² by using the SHELXTL program.²⁹ All non-hydrogen atoms and ions were refined anisotropically. The hydrogens bonded to carbon and nitrogen were positioned geometrically in accordance with hybridization and refined by using the riding model on the parent atoms. The hydrogen atoms bonded to oxygen were located from a Fourier difference map and refined with fixed isotropic parameters *U*_{iso}(H) = 1.5*U*_{iso}(O). During the refinement process, two badly disordered and diffused outer-sphere water molecules were found in the asymmetric units of both structures. Thereby, the SQUEEZE procedure from the PLATON program was used³⁰ to modify the intensities of reflections corresponding to disordered solvent molecules. Therefore, in the description of the crystal structure, magnetic, and spectroscopic studies, we have referred to the synthesized polymetallic complexes as 1 and 2 without the two weakly bound outer-sphere water molecules whose contribution was assumed to be minimal. Of the 18 resulting and coordinated-to-metal-centers water molecules, one must actually be present as an OH⁻ anion, an anion that is required to provide a charge neutral unit cell. Unfortunately, it has not proven possible to identify which of the “18” water molecules is actually an OH⁻ anion most likely because the loss of a hydrogen ion from water is either disordered among all the water present or perhaps from the two water molecules that, the refinement revealed, were disordered in the asymmetric units of both 1 and 2. Thus the structures have been refined with 18 water molecules, but the stoichiometry of each compound has been formulated as Na[Co₁₂(PMAS)₆(H₂O)₁₇(OH)] for 1 and Na[Ni₁₂(PMAS)₆(H₂O)₁₇(OH)] for 2 in order to keep charge balance between anions and metal cations. Crystal data, including the final residuals for structures 1 and 2, are shown in Table 1. Selected bond lengths and angles for both structures are presented in Tables S3 and S4 of the Supporting Information. These structures were checked for errors and inconsistencies using the PLATON software,³⁰ and respective reports are presented in the Supporting Information (S12, S13).

Magnetic Properties. The magnetic properties of complexes 1 and 2 have been measured on a Quantum Design MPLS XL-5 superconducting quantum interference magnetometer that was calibrated

with metallic palladium and pure $\text{CuSO}_4 \cdot 5\text{H}_2\text{O}$. For each measurement, the sample was zero-field cooled to 5 K, and the susceptibility was measured upon warming to 300 K in an applied field of 0.5 T. Complex **2** has also been studied a second time at 0.5 T and at 0.75 and 1.0 T. The observed molar magnetic susceptibilities have been corrected for the diamagnetic contribution of the constituents by subtracting -0.001295 emu/mol for both complexes, corrections that have been obtained from tables of Pascal's constants.⁴⁷

RESULTS AND DISCUSSION

Preparation. The syntheses of $\text{Na}[\text{Co}_{12}(\text{PMAS})_6(\text{H}_2\text{O})_{17}(\text{OH})] \cdot 2\text{H}_2\text{O}$, **1**·2H₂O, and its analogue $\text{Na}[\text{Ni}_{12}(\text{PMAS})_6(\text{H}_2\text{O})_{17}(\text{OH})] \cdot 2\text{H}_2\text{O}$, **2**·2H₂O, have been carried out by using a pH-dependent reaction between cobalt(II) and nickel(II) cations and H₄PMAS in aqueous solution. The pH of a 0.1 M aqueous solution of H₄PMAS is 2.73 and abruptly decreases to 1.70 upon the addition of the metal salts, a decrease that indicates the formation of the complex and the liberation of H⁺ ions into the solution. The pH adjustment to 5 for complete complexation was carried out by the dropwise addition of 1 M NaOH aqueous solution. Our studies indicated that any further increase in pH of the solutions of either the cobalt(II) or the nickel(II) cations leads to the precipitation of an amorphous species of irreproducible composition. The isolated complexes **1**·2H₂O and **2**·2H₂O obtained with a controlled pH synthesis are polynuclear complexes. It should be noted that some carboxyphosphonates similarly tend to form multinuclear complexes with different types of structures.^{1,20–23,26,31}

Spectroscopic Results. Solid samples of **1**·2H₂O and **2**·2H₂O in the form of ground polycrystallites have been studied by diffuse reflectance electronic spectroscopy, and their visible spectra are shown in Figure 1. Characteristic absorption bands

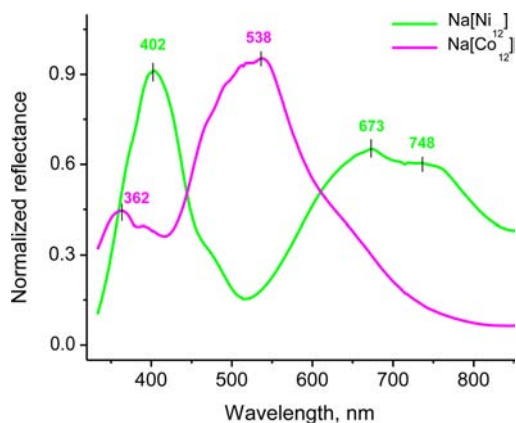


Figure 1. Diffuse reflectance spectra of solid complexes **1** and **2**.

for the d–d transitions of the cobalt(II) cation in a pseudo-octahedral environment are observed for complex **1**·2H₂O. Figure 1 shows asymmetric bands in the visible region of the spectrum that can be deconvoluted into several peaks of variable intensity (S17). These peaks can be attributed to two crystallographically different Co centers in complex **1**. There are numerous literature examples of possible spin-forbidden transitions for Co(II) complexes, transitions whose intensity are influenced by intensity stealing from a spin-allowed transition. Since we do not have ideal octahedral geometries in both crystallographically inequivalent Co centers, these transitions may involve split levels of ²G, ²H, ²D, and ²P terms for higher energy transitions, and the ²G term for lower energy ones. This possibility cannot be ruled out and also cannot be proved

unambiguously. The two predominant unresolved peaks in the spectrum at ca. 540 and 510 nm probably correspond to the ⁴T_{1g}(F) → ²T_{1g}(P) transitions of the two crystallographically inequivalent cobalt(II) cations found in **1**. Alternatively, the weak unresolved structure observed in the main absorption peak of **1** may result from a rather large spin–orbit coupling in the cobalt(II) ⁴T_{1g}(P) excited state, a coupling that removes the excited state degeneracy.³²

The diffuse reflectance spectrum of **2** also reveals similar characteristic absorption peaks for a nickel(II) cation, see Figure 1. The band at 402 nm may be assigned to the ³A_{2g} → ³T_{1g}(P) transition.^{33,34} The two somewhat less intense, partially resolved, peaks at ca. 670 and 750 nm are characteristic of the spin-allowed ³A_{2g} → ³T_{1g}(F) transition and the spin-forbidden ³A_{2g} → ¹E_g transition (S16). The specific assignment of these two peaks is tentative, but it is apparent that the spin-forbidden transition has gained intensity through an intensity stealing mechanism³⁴ mediated, at least in part, by the local distortion of the nickel(II) coordination environment.

The infrared spectra of complexes **1** and **2** exhibit characteristic peaks related to vibrational frequencies of the different functional groups found in the PMAS⁴⁻ anion. The frequencies corresponding to all donor sites are shifted in **1** and **2** as compared with those in the spectrum of the free ligand, a shift that clearly indicates the coordination of the PMAS⁴⁻ anion by the cobalt(II) and nickel(II) cations. The absorption peaks at 1622 cm⁻¹ and 1402 cm⁻¹ in **1** and 1628 cm⁻¹ and 1404 cm⁻¹ in **2** are assigned to asymmetric and symmetric stretching vibrations of the coordinated COO⁻ group, respectively. The differences, Δν, in the frequencies of the ν_s(COO⁻) and the ν_{as}(COO⁻) absorptions in **1** and **2** are 220 and 224 cm⁻¹, respectively. Large Δν values indicate the monodentate nature of the coordinated carboxyl group.³⁵ Absorptions in the range of 1136 to 1123 cm⁻¹ and 1080 to 923 cm⁻¹ are assigned to the asymmetric and symmetric stretching vibrations of the coordinated phosphonic moiety.³⁶ Both **1** and **2** also exhibit absorptions at 617 to 544 cm⁻¹ and 478 to 415 cm⁻¹, respectively, that may be assigned to ν(M–O) and ν(M–N) vibrations, respectively.³⁷ Broad absorptions in the 3600 to 3200 cm⁻¹ spectral region arise from the stretching vibrations of the water molecules and indicate the presence of extensive hydrogen-bonding in both **1** and **2**.

Thermogravimetric Analysis of Complexes. Both multinuclear complexes contain molecules of outer-sphere crystallate water, which continuously leaves the compounds after the beginning of sample heating in a nitrogen atmosphere. The endothermic dehydration ends after two distinctive stages at ~300 °C for **1** and ~325 °C for **2** (S9, S10), followed by decarboxylation of the ligand in the range of 300–500 °C. Calculated and observed weight losses are in good agreement (S11). Final products of anaerobic thermal decomposition of studied complexes are most likely composed of corresponding metal orthophosphates and metal oxides.

Structures of Complexes 1 and 2. Both **1** and **2** are isomorphous and crystallize in the rhombohedral crystal system with the R³ space group. As shown in Figure 2, the asymmetric units contains only 1/6 of the M₁₂(PMAS)₆ structures. These units form a dodecanuclear moiety centered on the sodium cation, which is a rather rare and peculiar feature. Thus, a search of the CCDC database on that subject has revealed only 12 entries (presented in S8) with two additional structures described in this paper. These include Na-centered compounds with carboxylic acids, phosphonic acids, and oximes/hydroxamic

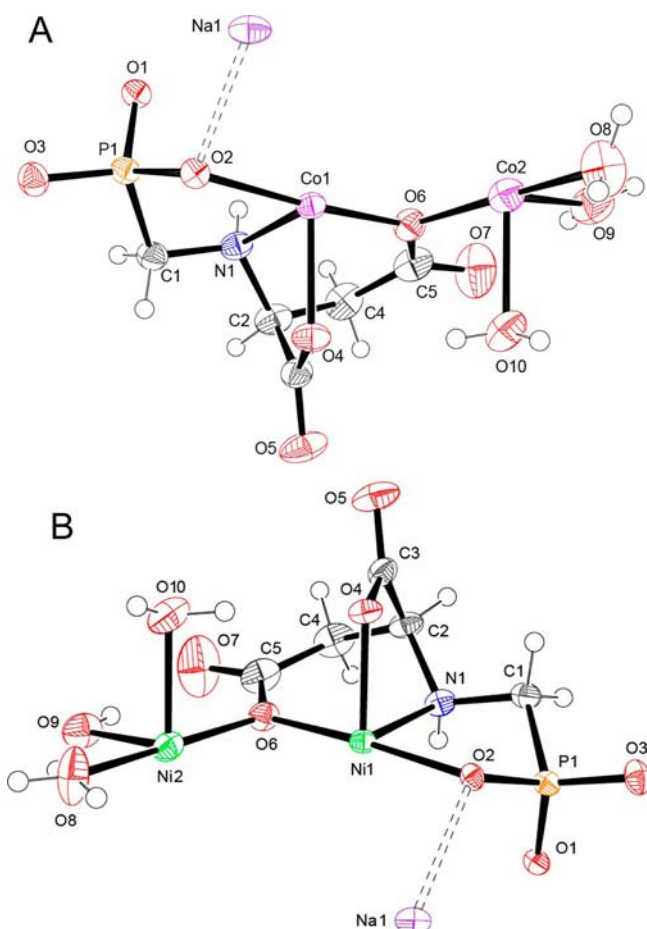


Figure 2. The asymmetric units of the $M_{12}(PMAS)_6$ portion of **1** (A) and **2** (B) shown with their respective numbering schemes. Thermal ellipsoids are drawn at 50% probability.

acids but exclude numerous crown-ethers and their derivatives (S8).

Because of their isomorphism, the discussion of the molecular and crystal structure of $Na[Co_{12}(PMAS)_6(H_2O)_{17}(OH)]$, **1**, and $Na[Ni_{12}(PMAS)_6(H_2O)_{17}(OH)]$, **2**, is combined. Na(1) in **1** and **2** occupies a special position on the 3-fold axis and is a center of symmetry of the molecule, see Figure 3. The sodium cation environment may thus be described as six-coordinated.^{38,39} As is shown in Figure 4, Na(1) is in a highly distorted trigonal-antiprismatic environment of crystallographically equivalent O(2) atoms with bond distances and angles presented in Tables S3 and S4. The Na(1)–O(2) bond distances are nearly identical for complexes **1** and **2** with values of 2.428(3) and 2.433(2) Å, respectively. A significant deviation of angles from $\sim 90^\circ$ in the coordination polyhedron of the Na(1) cation further confirms the assignment of its geometry as non-octahedral (S5, S6). The oxygen atom O(2) is a μ^3 -bridge connecting two symmetrically dependent Co(1) or Ni(1) cations with the Na(1) ion, forming tetrahedral angles for Co(1)–O(2)–Co(1) of $112.47(14)^\circ$ and Ni(1)–O(2)–Ni(1) of $114.72(10)^\circ$ and the close to normal angles for Co(1)–O(2)–Na(1) of $93.48(12)^\circ$, Ni(1)–O(2)–Na(1) of $94.11(8)^\circ$, Co(1)–O(2)–Na(1) of $92.91(11)^\circ$, and Ni(1)–O(2)–Na(1) of $93.17(8)^\circ$.

The Co(1) and Co(2) cations in **1** and the Ni(1) and Ni(2) cations in **2** are in a distorted octahedral environment of MNO_5 and MO_6 , respectively (Figure 5). The Ni–O bond lengths ranging between 2.012(3) and 2.137(2) Å and the Ni(1)–N(1)

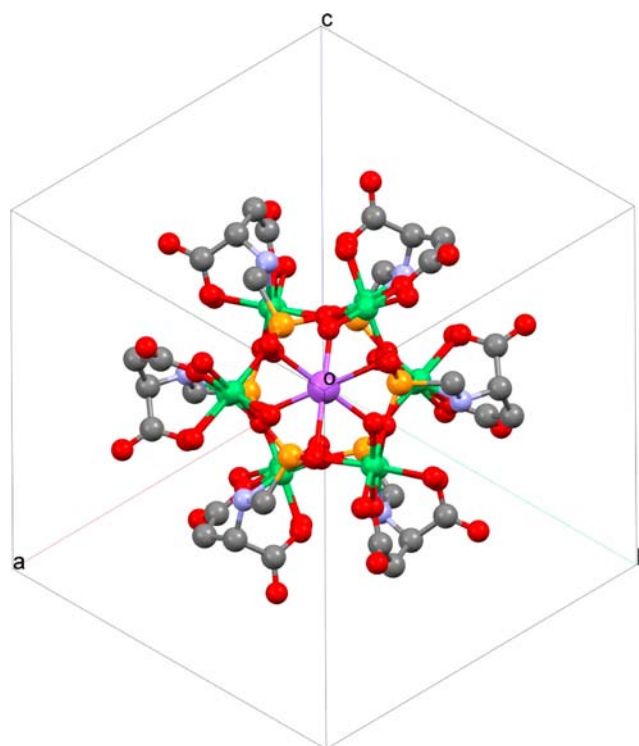


Figure 3. View of the unit cell content in the structure of **2** along [111] direction.

bond length of 2.062(3) Å are all in agreement with reported values for nickel(II) phosphonate complexes.⁴⁰ The equivalent bond distances for **1** are similar (S3, S4). The Co(1) and Co(2) cations in **1** and the Ni(1) and Ni(2) cations in **2** are connected by the μ^2 -bridging O(1) anions from the phosphonic group and O(6) anions from the carboxylic group at the edge of the coordination polyhedron. The Co(1)–Co(2) and Ni(1)–Ni(2) distances of 3.076(1) and 3.122(1) Å in **1** and **2** are significantly less than the sum of their van der Waals radii of ca. 4.6 Å and do not exclude the possibility of weak magnetic exchange interaction between these cations. The nature of the magnetic exchange pathways will be discussed below.

In both **1** and **2**, the coordination modes of $PMAS^{4-}$ to the M(1) and M(2) cations are implemented differently. The metal cation M(1) has two five-membered and one six-membered chelation rings, which share a M(1)–N(1) bond. Two of these rings, M(1)O(2)P(1)C(1)N(1) and M(1)N(1)C(2)C(4)C(5)–O(6) have a half-chair conformation. The third M(1)N(1)–C(2)C(3)O(4) ring has an envelope conformation, see Figure 2.

The $PMAS^{4-}$ ligand is coordinated to the M(1) cation by nitrogen N(1), O(2), O(4), and O(6) in a tetradentate fashion. The octahedral environment of the M(1) cation is completed by O(2A) and O(1A) from two neighboring $PMAS^{4-}$ ligands. The equatorial plane of the octahedron is occupied by one nitrogen, N(1), and three oxygens, O(4) from the α -carboxylate and O(2A) and O(1A) from two phosphonates of the $PMAS^{4-}$ -neighboring ligands, and the axial positions are occupied by the O(6) and O(2) oxygens from the β -carboxylic and phosphonic groups, respectively. It should be noted, that the axial M–O distances are different; one of the oxygens, O(6), is closer to the M(1) cation in the tetragonally distorted octahedron.

As mentioned earlier, there are two crystallographically different transition metals cations in each structure (Figure 5). The coordination environment of the M(2) cation consists of

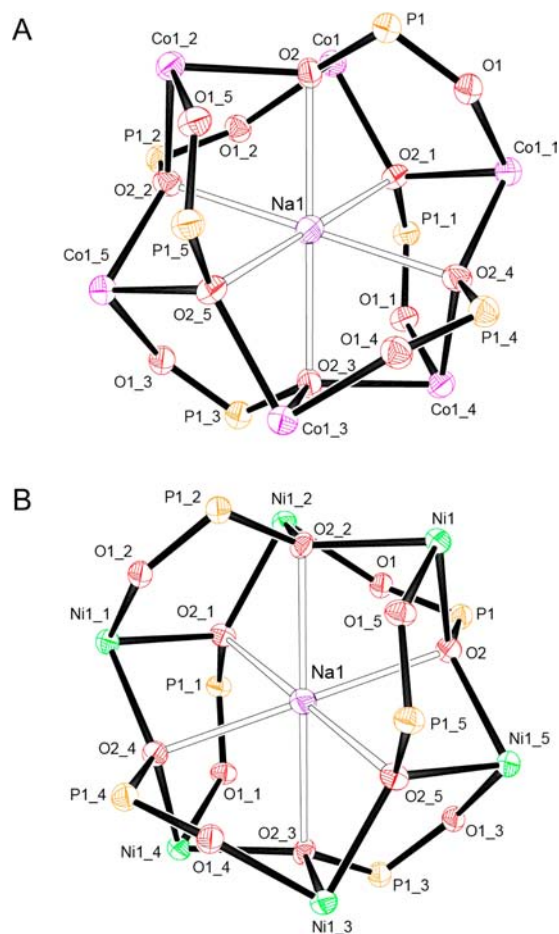


Figure 4. Coordination environment of Na⁺ in complexes 1 (A) and 2 (B).

three different PMAS⁴⁻ ligands and three water molecules. M(2) is six-coordinated by three bridging oxygens of PMAS⁴⁻, namely O(6) from the β -carboxylic group and O(1A) and O(3A) from two neighboring ligand phosphonic groups. The remaining three sites of the coordination environment are occupied by oxygens from three water molecules, O(8), O(9), and O(10), as is shown in Figure 5. Single, C(3)–O(4) and C(5)–O(6), and double, C(3)–O(5) and C(5)–O(7), bonds for both carboxylic groups of the ligand are clearly localized (S3, S4). The phosphonic groups have a tetrahedral structure with a localized double bond, P(1)–O(3) (S3, S4).

Unfortunately, as noted above, it has proven impossible to distinguish the single OH⁻ counterion from the numerous water molecules in the solid-state structures of 1 and 2. A similar difficulty has been reported for some carbohydrate metal–organic framework compounds⁴¹ and in the Fe(III) hydroxamate complex.⁵⁸ Moreover, an extensive three-dimensional network of hydrogen bonds is present in the crystal structures of 1 and 2. The hydrogen bond parameters for the disordered water molecules in the crystal structures could not be determined.

Complexes 1 and 2 form a three-dimensional structure with central one-dimensional channels along the 3-fold crystallographic axis. The sodium ion occupies the center of the cavity and hence creates a 24-member macrocycle, see Figure 4. Such a “filled” macrocyclic structure has also been observed for K₂[Co(PMIDA)]₆·xH₂O, where the 24-member cycle contains a water molecule in its center.²⁰ It is interesting to note in this context that several other Na-centered large transition metal

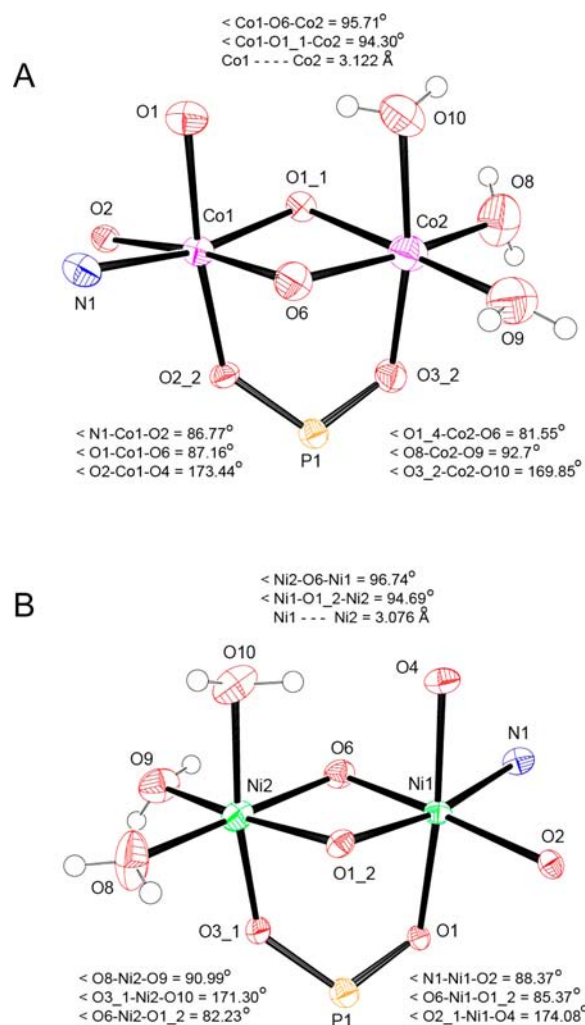


Figure 5. Coordination polyhedrons of Co(II), 1, (A) and Ni(II), 2, (B). Shown are three bridges between different metal centers: via O6 of the carboxylic group and oxygen atoms of phosphonate groups (O1 and O3).

complexes crystallize in the same $R\bar{3}$ space group with alkali metal being in a special position on a 3-fold axis.^{39,58} The formation of similar metallacycles with the O–P–O bridge has been described for several metal phosphonates.^{22,26,42–44}

The volume of the cavity is calculated by assuming a cylinder with an axis passing through the Na(1) cation and coinciding with the 3-fold axis. The radius of the cylinder is the length of the perpendicular to the 3-fold axis to one of the M(2) cations. The cylinders have diameters of 6.208 and 6.136 Å and heights of 7.705 and 7.589 Å and hence volumes of 233.2 and 224.4 Å³ for 1 and 2, respectively. These large cavities are produced by a very favorable spatial superposition of the numerous ligand donor atoms.

Packing diagrams for complexes 1 and 2 can be found in S14 and S15, respectively. Both compounds form loose structures that resemble those for metal–organic frameworks or extended ball-shaped carbon nanoassemblies. Thus, the cell volume for 1 is 2172.2 Å³ with the structure occupying 1288.5 Å³ (59.3%), while for 2, the cell volume is 2144.4 Å³ with the structure occupying only 1240.7 Å³ (57.9%).

Literature data about structures of other known polymetallic multinuclear complexes that contain phosphono-(amino-carboxylic) acids and some diphosphonic acids are summarized in Table

Table 2. Binding Modes and Structural Features in Some Poly(multi)metallic Complexes of Phosphono-Amino(carboxylic) Acids, Aminophosphonates, and Phosphonates

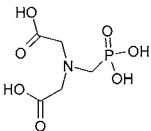
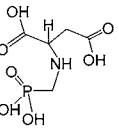
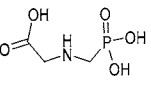
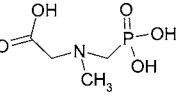
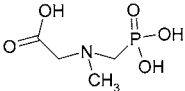
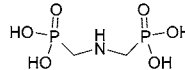
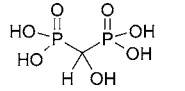
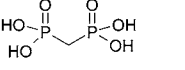
Ligand	Compound or complex ion	Core, comments	L Binding Mode	Ref.	
H₄PMIDA : 	[Co ₁₅ (PMIDA) ₆ (BTC) ₂ (H ₂ O) ₁₂ ·6H ₂ O	Metal centered CoCo ₂ Co ₆ Co ₆ pseudospherical unit	bridging COO ⁻ and PO ₃ ⁻ groups	50	
	[Co ₁₅ (PMIDA) ₆ (H ₂ O) ₂₄][trans-E]·xH ₂ O [Co ₁₅ (PMIDA) ₆ (cisH ₃ E) ₂ (H ₂ O) ₁₈ ·12H ₂ O	Metal centered CoCo ₂ Co ₆ Co ₆ pseudospherical nanoclusters			51
	{[Gd ₆ Ni ₃ (PMIDA) ₆ (H ₂ O) ₁₇ ·(H ₂ O) ₂₅]} <i>n</i>	Gd ₆ Ni ₃ clusters linked by Gd ³⁺ ion	bridging COO ⁻ and PO ₃ ⁻ groups		52
	M _x [Fe(PMIDA)] ₆ · <i>n</i> H ₂ O M= Na, K, Rb	M-O-P-O-M -bridged bridging cyclic hexamer			23
	K ₂ [Co(PMIDA)] ₆ ·xH ₂ O	M-O-P-O-M -bridged cyclic hexamer; disordered water molecules inside the cavity	bridging PO ₃ ⁻ group		20
	(H ₃ O) ₈ [Ni ₄ O ₂ (HPMIDA) ₄ (H ₂ O) ₂]	16 membered metalo- macrocycle	bridging COO ⁻ groups		26
	[Co ₄ (H ₂ O) ₄ (HPMIDA) ₂ (PMIDA) ₂ ·2H ₂ O	16 membered metalo- macrocycle	bridging COO ⁻ groups		22
	[Cu ₂ M ₂ (PMIDA) ₂ (H ₂ O) ₆]·3H ₂ O (M= Mn, Co, Cd), [Cu ₂ Ln ₂ (PMIDA) ₂ (C ₂ O ₄)(H ₂ O) ₃]·3.5H ₂ O (Ln= La, Nd)	alternating Cu and M ions result in the formation of double-layered blocks	bridging COO ⁻ and PO ₃ ⁻ groups		53
Mn(H ₂ O)(PMIDA)	M-O-P-O-M -bridged chains linked by COO ⁻ groups into 2D rectangular grid of 24-membered cycles	bridging COO ⁻ and PO ₃ ⁻ groups		27	
H₄PMAS 	Na[M ₁₂ (PMAS) ₆ (H ₂ O) ₁₇]OH (M = Co ²⁺ , Ni ²⁺)	[MO ₅ N] units and Na[MO ₆]-cations form Na-centered cage	bridging COO ⁻ and PO ₃ ⁻ groups, N-binding as well	this work	
H₃PMG : 	Cd ₉ (PMG) ₆ (H ₂ O) ₁₂ ·6H ₂ O	M-O-P-O-M -bridged cyclic cluster		54	
MeH₃PMG = L 	Cd ₉ L ₆ (H ₂ O) ₁₂ ·19H ₂ O	bis-μ-P(O)-groups bridge three linked Cd units	bridging COO ⁻ and PO ₃ ⁻ groups	55	

Table 2. continued

Ligand	Compound or complex ion	Core, comments	L Binding Mode	Ref.
MeH₃PMG = L 	$\{\text{Zn}_7\text{L}_6\} \{\text{Ni}(\text{bipy})(\text{H}_2\text{O})_4\}_2 \cdot 16\text{H}_2\text{O}$ $[\text{H}_3\text{O}]\{\text{Zn}_7\text{L}_6\} \{\text{Ni}(\text{H}_2\text{O})_2(\text{bipy})_2\} 1.5 \cdot 12\text{H}_2\text{O}$ $\{\text{Zn}_6\text{L}_6(\text{Zn})\} \{\text{Zn}(\text{H}_2\text{O})_6\}_2 \cdot 22\text{H}_2\text{O}$	Metal centered ZnZn ₆ unit	M-O-P-O-M cyclic cluster	31
NH(CH₂PO₃H₂)₂ = L 	$\text{Cu}_4\text{L}_2(4,4'\text{-bipy})(\text{H}_2\text{O})_4 \cdot 9\text{H}_2\text{O}$	Cu_2O_2 -phosphonate dimeric units form a chains interconnected into a 2D grid layer	$\mu\text{-PO}_3\text{-M}_3$ bridged	56
HOCH(PO₃H₂)₂ = L 	$\text{Na}_2\text{Cu}_{15}(\text{L})_6(\text{OH})_2(\text{H}_2\text{O})$	mixed-valence Cu(I/II) compound; honeycomb layer of edge-sharing Cu ₃ L ₃ triangles that form 24-membered rings; 18-membered ring for centrosymmetric Cu ₃ L ₃ cluster	M-O-P-O-M bridged cyclic cluster	38
CH₂(PO₃H₂)₂ = L 	$(\text{enH}_2)_4[\text{Mo}_7\text{O}_{16}(\text{L})_3] \cdot 7\text{H}_2\text{O}$ $(\text{ppzH}_2)_4[\text{Mo}_7\text{O}_{16}(\text{L})_3] \cdot 8\text{H}_2\text{O}$	Metal centered Mo ^V ₆ Mo ^{VI} (spiro poly-cyclic) cluster anion	tetrakis-M-O-P-O-M and tris-M-O-M bridged cluster	57

2. Structures and properties of some large transition metals complexes with simpler phosphonic and carboxylic acids were recently published.^{48,49} A substantial group of better known and studied homo- and heterometallic polynuclear complexes with other than phosphorus-containing organic ligands (such as, for example, carboxylic acids, aldoximes, aminoalcohols, etc.) was out of the scope of our investigation.

One of the prime interests in large polymetallic multinuclear complexes is a search for single molecule magnets which may have interesting practical applications in the miniaturization of electronic devices and data storage media.

Magnetic Properties of the 1. Both temperature dependence of the inverse molar magnetic susceptibility, $1/\chi_M$, and of $\chi_M T$ for complex **1** are shown in Figure 6; the inverse molar susceptibility is linear between 50 and 300 K and yields a Weiss temperature of -22 K, a Curie constant of 41.09 emu K/mol, and a corresponding effective magnetic moment, μ_{eff} of 18.13 μ_B per mole or 5.23 μ_B per mole of cobalt. Further, a plot of μ_{eff} indicates that the moment decreases slightly from 5.06 μ_B per mole of cobalt at 300 K to 4.46 μ_B at 50 K and then decreases substantially to 2.28 μ_B at 5 K; the corresponding $\chi_M T$ decreases continuously from 38.39 emu K/mol at 300 K to 7.77 emu K/mol at 5 K.

The decrease in $\chi_M T$, and especially the decrease observed below 50 K, could be the result of either spin-orbit coupling of the $S = 3/2$ ground state of the cobalt(II) ions or the presence of intramolecular antiferromagnetic exchange interactions between the cobalt(II) ions in the Co₁₂ complex. All attempts to fit $\chi_M T$, either between 5 and 300 K or 5 and 50 K with $S = 3/2$ in the presence of spin-orbit coupling,⁴⁵ yield either very poor fits or implausible fit parameters, and one is forced to conclude that if spin-orbit coupling is present, it is too small to produce the observed temperature dependence of $\chi_M T$. Thus, one must consider magnetic exchange interactions within the Co₁₂ cluster.

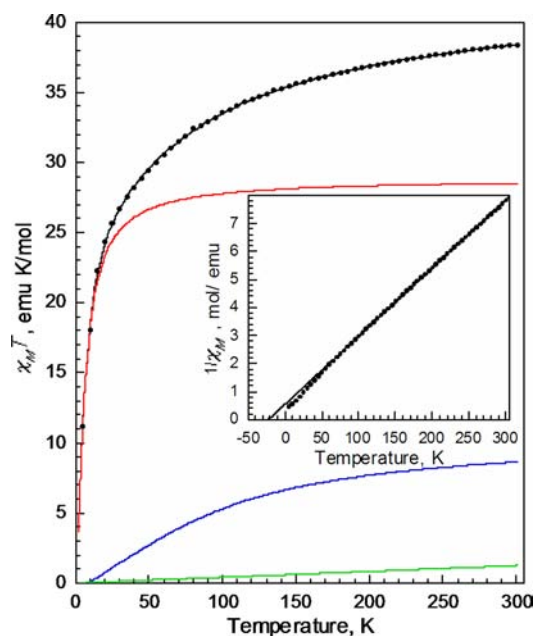


Figure 6. The temperature dependence of $\chi_M T$ obtained at 0.5 T for complex **1** and the best fit between 5 and 300 K, black line, obtained with $S_1 = S_2 = 3/2$, $J_1 = -15.3(7)$ cm^{-1} for the Co(1)⋯Co(1) exchange pathway, blue line; $J_2 = -1.06(2)$ cm^{-1} for the Co(1)⋯Co(2) exchange pathway, red line; $g_1 = 2.38(3)$ for Co(1), $g_2 = 3.06(2)$ for Co(2), and the average $N\alpha = 0.00030(15)$ emu/mol per cobalt ion, green line. Inset: The temperature dependence of $1/\chi_M$ with a Curie-Weiss law fit between 50 and 300 K, black line.

A study of the structure of **1** reveals that it consists of rather well separated tetrameric nonlinear chains, Co(2)⋯Co(1)#4⋯Co(1)

#3...Co(2)#3, of divalent cobalt(II) ions with nonbonded Co(2)...Co(1), Co(1)...Co(1)#4, Co(2)...Co(2)#1, and Co(2)...Co(2) distances of 3.122, 3.563, 3.580, and 8.307 Å, respectively, and a dihedral angle of 175°. Thus there are two potential superexchange pathways between the four cobalt(II) ions that could lead to effective antiferromagnetic exchange.

The first, and perhaps more significant, exchange pathway involves the two pairs of Co(1)...Co(2) ions which have two superexchange bridging pathways, Co(1)–O(1)–Co(2) and Co(1)–O(6)–Co(2), with bridging angles of 94.3(1)° and 95.7(1)°, respectively; the corresponding through bond superexchange distances are 4.256(6) Å for the Co(1)–O(1)–Co(2) pathway and 4.209(8) Å for the Co(1)–O(6)–Co(2) pathway, and thus the bonding environment might be expected to yield a weak antiferromagnetic exchange interaction that can be fit between 5 and 300 K with the Heisenberg exchange Hamiltonian, $H = -2JS_1S_2$, with $S_1 = S_2 = 3/2$. However, a fit of $\chi_M T$ yields only marginally acceptable fits with a rather high and unreasonable second-order Zeeman contribution, $N\alpha$, to the molar magnetic susceptibility.

Thus, one must also consider the second intramolecular exchange interaction within the tetramer involving one Co(1)...Co(1)#5 interaction. This second interaction has a single superexchange bridging pathway, Co(1)–O(2)–Co(1)#5, with a bridging angle of 112.47(14)°; the corresponding through bond superexchange distance is 4.285 Å, and this bonding environment may also be expected to produce a weak antiferromagnetic exchange interaction. Thus, $\chi_M T$ for the Co₁₂ complex has been fit between 5 and 300 K with the above Hamiltonian with $S_1 = S_2 = 3/2$ and two exchange coupling parameters, J_1 for the one Co(1)...Co(1)#5 exchange pathway and J_2 for the two Co(1)...Co(2) exchange pathways with contributions in a 1 to 2 ratio and with two g values, g_1 for Co(1) and g_2 for Co(2). The resulting best fit, see Figure 6, yields $g_1 = 2.38(3)$, $g_2 = 3.06(2)$, $J_1 = -15.3(7)$ cm⁻¹, $J_2 = -1.06(2)$ cm⁻¹, and an average $N\alpha = 0.00030(15)$ emu/mol of cobalt ion. An alternative fit with an average g value for the two crystallographically inequivalent cobalt(II) ions yields a similar but slightly poorer fit. However, fits with the alternate 2 to 1 ratio for J_1 and J_2 are unacceptable. The fitting parameters for the various fits are given in S7.

Magnetic Properties of 2. Both the inverse molar magnetic susceptibility, $1/\chi_M$, and $\chi_M T$ of the Ni₁₂ complex **2** are shown in Figure 7; the inverse molar magnetic susceptibility is linear between 100 and 300 K and yields a Weiss temperature of 4.8 K, a Curie constant of 12.99 emu K/mol, and a μ_{eff} of 10.19 μ_B per mole or 2.94 μ_B per mole of nickel. Further, a plot of μ_{eff} indicates that the moment increases slightly from 2.93 μ_B per mole of nickel(II) at 300 K to 2.97 μ_B at 50 K and then decreases to 1.66 μ_B at 5 K; the corresponding $\chi_M T$ increases slightly from 13.24 emu K/mol at 300 K to 13.47 emu K/mol at 100 K and then decreases continuously to 4.14 emu K/mol at 5 K.

The small increase in the moment between 300 and 100 K is most likely due to spin–orbit coupling within the ²E_g electronic ground states of the two crystallographically nonequivalent pseudo-octahedral nickel(II) ions.⁴⁶ This small increase will not be considered in the following discussion of the magnetic exchange interactions in complex **2**.

The structure of **2** reveals that it consists of rather well separated tetrameric nonlinear chains, Ni(2)#1...Ni(1)#1...Ni(1)#4...Ni(2)#4, of divalent nickel(II) ions with nonbonded Ni(1)...Ni(2), Ni(1)...Ni(1)#4, and Ni(2)...Ni(2)#4 distances of 3.076, 3.548, and 8.186 Å, respectively, and a

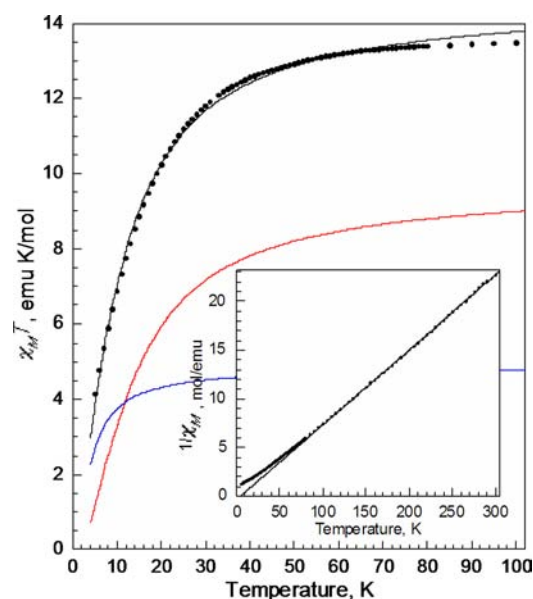


Figure 7. The temperature dependence of $\chi_M T$ obtained at 0.5 T for **2** and the best fit between 5 and 100 K, black line; obtained with $S_1 = S_2 = 1$, $J_1 = -1.17(6)$ cm⁻¹ for the Ni(1)...Ni(1) exchange pathway, blue line; $J_2 = -4.00(8)$ cm⁻¹ for the Ni(1)...Ni(2) exchange pathway, red line; and $g = 2.209(2)$. $N\alpha$ was constrained to zero. Inset: The temperature dependence of $1/\chi_M$ with a Curie–Weiss law fit between 100 and 300 K, black line.

dihedral angle of 174°. Thus there are two potential superexchange pathways between the four nickel(II) ions that could lead to effective antiferromagnetic exchange. The first, and probably more significant, pathway involves the two pairs of Ni(1)...Ni(2) ions which have two superexchange bridging pathways, Ni(1)–O(1)–Ni(2) and Ni(1)–O(6)–Ni(2), with bridging angles of 94.7(1)° and 96.7(1)°, respectively. The corresponding through bond superexchange distances are 4.181(6) Å for the Ni(1)–O(1)–Ni(2) pathway and 4.115(8) Å for the Ni(1)–O(6)–Ni(2) pathway, and thus the bonding environment may be expected to yield a weak antiferromagnetic exchange interaction that can be fit between 5 and 300 K with the above exchange Hamiltonian with $S_1 = S_2 = 1$. However, a fit of $\chi_M T$ yields only marginally acceptable fits with a high and unreasonable second-order Zeeman contribution, $N\alpha$, to the molar magnetic susceptibility.

Thus, one must again also consider the second intramolecular exchange interaction within the tetramer involving one Ni(1)...Ni(1)#4 interaction. This second interaction has a single superexchange bridging pathway, Ni(1)–O(2)–Ni(1), with a bridging angle of 114.7(1)°. The corresponding through bond superexchange distance is 4.213(4) Å, and this bonding environment may again be expected to produce a weak antiferromagnetic exchange interaction. Thus, the $\chi_M T$ for complex **2** has been fit between 5 and 300 K with the above Hamiltonian with $S_1 = S_2 = 1$ and two exchange coupling parameters, J_1 for the one Ni(1)...Ni(1)#4 exchange pathway and J_2 for the two Ni(1)...Ni(2) exchange pathways with contributions in a 1 to 2 ratio and with one g value for Ni(1) and Ni(2). The resulting best fit, see Figure 7, yields $g = 2.209(2)$, $J_1 = -1.17(6)$ cm⁻¹, and $J_2 = -4.00(8)$ cm⁻¹. $N\alpha$ was found to be essentially zero and was subsequently constrained to zero. Because, in the case of **2**, the J_1 and J_2 values are closer to each other in value, a fit with the alternate 2 to 1 ratio for J_1 and J_2 is almost as good as the best fit (S7).

It may be noted that the antiferromagnetic exchange coupling is weaker in **2** than in **1** even though the former has, as expected, slightly shorter through-bond superexchange distances and rather similar oxygen bridging angles. Unfortunately, such comparisons may be of limited value because of the very different temperature ranges of the fitted data.

CONCLUSIONS

A new structural isomer of *N*-(phosphonomethyl)iminodiacetic acid (H_4PMIDA), namely *N*-(phosphonomethyl)aminosuccinic acid, $H_2O_3PCH_2NHCH(COOH)CH_2COOH$, herein labeled as H_4PMAS , has been synthesized and characterized. The lower symmetry of H_4PMAS , as compared with H_4PMIDA , removes the structural equivalence of portions of the ligand and, thus, facilitates the formation of coordination compounds of unusual geometry.

Two new isostructural carboxyphosphonate complexes, $Na[Co_{12}(PMAS)_6(H_2O)_{17}(OH)]$, **1**, and $Na[Ni_{12}(PMAS)_6(H_2O)_{17}(OH)]$, **2**, with an unusual dodecanuclear architecture with encapsulated sodium ions have been prepared and characterized using spectroscopic methods, variable temperature magnetochemistry, X-ray, and thermal analyses. The molecular structure of these isomorphous complexes contains a 24-membered macrocycle that creates a cylindrical cavity containing octahedrally coordinated sodium cations.

The self-assembly process in aqueous solution containing transition metal carboxyphosphonates and sodium cations led to host-guest interactions between the quasi-macrocycle formed by six ligand-bimetallic units and the exogenous sodium cation. The unique cavity is produced by a favorable spatial superposition of the numerous donors of bridging ligands. The crystal structures of **1** and **2** also have a complex three-dimensional network of hydrogen bonds. Because there are only a few examples of polynuclear carboxyphosphonate complexes, the present $PMAS^{4-}$ complexes provide a new approach for the design of unusual molecular architectures.

Both **1** and **2** are paramagnetic complexes at high temperatures and exhibit weak antiferromagnetic exchange interactions at low temperatures. Enhanced exchange interactions may result in future homo- or heterometallic complexes with related phosphonate ligands.

ASSOCIATED CONTENT

Supporting Information

Potentiometric data for the ligand, H_4PMAS (S1, S2); tables of selected bond lengths and valence angles for **1** (S3) and **2** (S4); details of geometry of coordination polyhedrons of Na^+ in structures of **1** (S5) and **2** (S6); results of the best fit of magnetochemical data for both complexes (S7); structures of known sodium-centered polymetallic complexes with oximes/hydroxamic acids, carboxylic acids, and phosphonic acids (S8); data of TG/DTA analysis for complexes **1** and **2** (S9–S11); checkCIF reports for **1** (S12) and **2** (S13); crystal packing diagrams for **1** (S14) and **2** (S15); full line shape analysis of the reflectance spectra in the visible region for **1** (S16) and **2** (S17). This material is available free of charge via the Internet at <http://pubs.acs.org>. A complete set of crystallographic information for $Na[Co_{12}(PMAS)_6(H_2O)_{17}(OH)]$, **1**, and for $Na[Ni_{12}(PMAS)_6(H_2O)_{17}(OH)]$, **2**, have been deposited with the Cambridge Crystallographic Data Centre database under the numbers 802284 and 802283.

AUTHOR INFORMATION

Corresponding Author

*Phone: 1-(417) 836-5165. E-mail: andriy.gudima@yahoo.com; glong@mst.edu, NN Gerasimchuk@MissouriState.edu.

Notes

The authors declare no competing financial interest.

ACKNOWLEDGMENTS

The authors thank Vladimir V. Bon' for his help with X-ray crystallography measurements and for various discussions and Prof. Vladimir Kolesnichenko (Xavier University, New Orleans, LA) for thermogravimetric studies. N.G. is also grateful to Dr. Kartik Ghosh for help with measurements of magnetic susceptibility.

REFERENCES

- (1) Cabeza, A.; Aranda, M. A. G. In *Metal Phosphonate Chemistry: From Synthesis to Applications*; Clearfield, A., Demadis, K., Eds.; The Royal Society of Chemistry: Cambridge, U. K., 2012; pp 107–132.
- (2) Nowack, B.; VanBriesen, J. M. *Biogeochemistry of Chelating Agents*, ACS Symposium Series; American Chemical Society: Washington, DC, 2005.
- (3) Clearfield, A. *Progress in Inorganic Chemistry*; Karlin, K. D., Ed.; Wiley: New York, 1998; Vol. 47, pp 371–510.
- (4) Franz, J. E.; Mao, M. K.; Sikorski, J. A. *Glyphosate: A Unique and Global Herbicide*, ACS Monograph No. 189; American Chemical Society: Washington, DC, 1997.
- (5) Kiss, T.; Lazar, I.; Kafarski, P. *Metal-Based Drugs* **1994**, *1*, 247–264.
- (6) Nowack, B. *Phosphorus in Environmental Technology: Principles and Application*; Valsami-Jones, E., Ed.; IWA Publishing: London, 2004; pp 147–173.
- (7) Anderegg, G.; Arnaud-Neu, F.; Delgado, R.; Felcman, J.; Popov, K. *Pure Appl. Chem.* **2005**, *77*, 1445–1495.
- (8) Clearfield, A. *Curr. Opin. Solid. State Mater. Sci.* **2002**, *6*, 495–506.
- (9) Motekaitis, R. J.; Martell, A. E. *J. Coord. Chem.* **1985**, *14*, 139–149.
- (10) Dhansay, M. A.; Linder, P. W. *J. Coord. Chem.* **1993**, *28*, 133–145.
- (11) Popov, K.; Rönkkömäki, H.; Lajunen, L. H. *J. Pure Appl. Chem.* **2001**, *73*, 1641–1677.
- (12) Dyatlova, N. M.; Tyomkina, V. Ya.; Popov, K. I. *Complexones and Complexonates*; Khimiya: Moscow, 1988.
- (13) Clarke, E. T.; Rudolf, P. R.; Martell, A. E.; Clearfield, A. *Inorg. Chim. Acta* **1989**, *164*, 59–63.
- (14) Han, G.-F.; Luo, H.-Z.; Ye, Q.; Xiong, R. G. *Z. Anorg. Allg. Chem.* **2008**, *634*, 1991–1995.
- (15) Heineke, D.; Franklin, S. J.; Raymond, K. N. *Inorg. Chem.* **1994**, *33*, 2413–2421.
- (16) Menelaou, M.; Dakanali, M.; Raptopoulou, C. P.; Drouza, C.; Laloti, N.; Salifoglou, A. *Polyhedron* **2009**, *28*, 3331–3339.
- (17) Mao, J.-G.; Wang, Z.; Clearfield, A. *New J. Chem.* **2002**, *26*, 1010–1014.
- (18) Song, J. L.; Mao, J.-G.; Sun, Y.-Q.; Zeng, H.-Y.; Kremer, R. K.; Clearfield, A. *J. Solid State Chem.* **2004**, *177*, 633–641.
- (19) Mateescu, A.; Gabriel, C.; Raptis, R. G.; Baran, P.; Salifoglou, A. *Inorg. Chim. Acta* **2007**, *360*, 638–648.
- (20) Gutschke, S. O. H.; Price, D. J.; Powell, A. K.; Wood, P. T. *Angew. Chem., Int. Ed.* **1999**, *38*, 1088–1090.
- (21) Mao, J.-G.; Clearfield, A. *Inorg. Chem.* **2002**, *41*, 2319.
- (22) Fan, Y.; Li, G.; Jian, W.; Wang, M. U. L.; Tian, Zh.; Song, T.; Feng, Sh. *J. Solid State Chem.* **2005**, *178*, 2267–2273.
- (23) Cave, D.; Coomer, F. C.; Molinos, E.; Klauss, H.-H.; Wood, P. T. *Angew. Chem., Int. Ed.* **2006**, *45*, 803–806.
- (24) Mateescu, A.; Raptopoulou, C. P.; Terzis, A.; Tangoulis, V.; Salifoglou, A. *Eur. J. Inorg. Chem.* **2006**, 1945–1956.
- (25) Shi, F. N.; Almeida Paz, F. A.; Trindade, T.; Rocha, J. *Acta Crystallogr., Sect. E: Struct. Rep. Online* **2006**, *62*, m335–m338.
- (26) Ma, K.-R.; Xu, J.-N.; Ning, D.-K.; Shi, J.; Zhang, D.-J.; Fan, Y.; Song, T.-Y. *Inorg. Chem. Commun.* **2009**, *12*, 119–121.

- (27) Fan, Y.; Li, G.; Shi, Zh.; Zhang, D.; Xu, J.; Song, T.; Feng, Sh. *J. Solid State Chem.* **2004**, *177*, 4346–4350.
- (28) Soloshonok, V. A.; Belokon', Yu. N.; Kuzmina, N. A.; Maleev, V. I.; Svistunova, N. Yu. *J. Chem. Soc., Perkin Trans.* **1992**, *1*, 1525–1530.
- (29) SADABS; SAINT; SHELXTL; SMART; Bruker AXS Inc.: Madison, WI, 2003.
- (30) Spek, A. L. *PLATON*; Utrecht University: Utrecht, The Netherlands, 2010.
- (31) Lei, C.; Mao, J.-G.; Sun, Y.-Q.; Zeng, H.-Y.; Clearfield, A. *Inorg. Chem.* **2003**, *42*, 6157–6159.
- (32) Lever, A. B. P. *Inorganic Electronic Spectroscopy*, 2nd ed.; Elsevier: Amsterdam, 1984.
- (33) González, E.; Rodrigue-Witchel, A.; Reber, C. *Coord. Chem. Rev.* **2007**, *251*, 351–363.
- (34) Sacconi, L.; Mani, F.; Bencini, A. In *Comprehensive Coordination Chemistry*; Wilkinson, G., Gillard, R. D., McCleverty, J. A., Eds.; Pergamon Press: Oxford, 1987; Vol. 5, pp 2–347.
- (35) Deacon, G. B.; Phillips, R. J. *Coord. Chem. Rev.* **1980**, *33*, 227–250.
- (36) Piccolo, A.; Celano, G. *Environ. J. Sci. Health* **1993**, *B 28*, 447–457.
- (37) Nakamoto, K. *Infrared and Raman Spectra of Inorganic and Coordination Compounds*; Wiley: New York, 1986.
- (38) Zheng, L.-M.; Duan, C.-Y.; Ye, X.-R.; Zhang, L.-Y.; Wang, C.; Xin, X.-Q. *J. Chem. Soc., Dalton Trans.* **1998**, 905–908.
- (39) Gerasimchuk, N. N.; Dalley, N. K. *J. Coord. Chem.* **2004**, *57*, 1431–1445.
- (40) Poznyak, A. L.; Antsyshkina, A. S.; Sadikov, G. G.; Sergienko, V. S.; Stopolyanskaya, L. V. *Russ. J. Inorg. Chem.* **1998**, *43*, 961–970.
- (41) Forgan, R. S.; Smaldone, R. A.; Gassensmith, J. J.; Furukawa, H.; Cordes, D. B.; Li, Q.; Wilmer, C. E.; Botros, Y. Y.; Snurr, R. Q.; Slawin, A. M. Z.; Stoddart, J. F. *J. Am. Chem. Soc.* **2012**, *134*, 406–417.
- (42) Bideau, J. Le.; Payen, C.; Palvadeau, P.; Bujoli, B. *Inorg. Chem.* **1994**, *33*, 4885–4890.
- (43) Maeda, K. *Microporous Mesoporous Mater.* **2004**, *73*, 47–55.
- (44) Shi, F.-N.; Paz, F. A. A.; Trindade, T.; Rocha, J. *Acta Crystallogr., Sect. E: Struct. Rep. Online* **2006**, *62*, m335.
- (45) Kahn, O. *Molecular Magnetism*; VCH Publishers: New York, 1993; p 38.
- (46) Figgis, B. N. *Introduction to Ligand Fields*; Wiley-Interscience: New York, 1966.
- (47) Bain, G. A.; Berry, J. F. *J. Chem. Educ.* **2008**, *85*, 532–536.
- (48) Brechin, E. K.; Coxall, R. A.; Parkin, A.; Parsons, S.; Tasker, P. A.; Winpenny, R. E. P. *Angew. Chem., Int. Ed.* **2001**, *40*, 2700–2703.
- (49) Langley, S.; Helliwell, M.; Sessoli, R.; Teat, S. J.; Winpenny, R. E. P. *Inorg. Chem.* **2008**, *47*, 497–507.
- (50) Wang, X.-R.; Jia, Q.-X.; Liu, Z.-H. *Inorg. Chem. Commun.* **2012**, *15*, 281–284.
- (51) Gu, Z.-G.; Sevov, S. C. *Inorg. Chem.* **2009**, *48*, 8066–8088.
- (52) Zhuang, G.-L.; Jin, Y.-Ch.; Zhao, H.-X.; Kong, X.-J.; Long, L.-Sh.; Huang, R.-B.; Zheng, L.-S. *Dalton Trans.* **2010**, *38*, 5077–5079.
- (53) Gu, Z.-G.; Sevov, S. C. *J. Mater. Chem.* **2009**, *19*, 8442–8447.
- (54) Ramstedt, M.; Norgren, C.; Sheals, J.; Boström, D.; Sjöberg, S.; Persson, P. *Inorg. Chim. Acta* **2004**, *357*, 1185–1192.
- (55) Lei, Ch.; Mao, J.-G.; Sun, Y.-Q.; Dong, Zh.-Ch. *Polyhedron* **2005**, *24*, 295–303.
- (56) Yang, B. P.; Prosvirin, A. V.; Zhao, H.-H.; Mao, J.-G. *J. Solid State Chem.* **2006**, *179*, 175–185.
- (57) Dumas, E.; Sassoie, C.; Smith, K. D.; Sevov, S. C. *Inorg. Chem.* **2002**, *41* (15), 4029–4032.
- (58) Golenya, I. A.; Gumienna-Kontecka, E.; Boyko, A. N.; Haukka, M.; Fritsky, I. O. *Dalton Trans.* **2012**, *41*, 9427–9430.